ACS OMEGA

Open Access

http://pubs.acs.org/journal/acsodf

Article

Ergothioneine Stimulates Ca^{2+}-Mediated Brain-Derived Neurotrophic Factor Expression in NE-4C Nerve Cells

Caiyue Shi, Sumire Asaba, Saya Nakamura, and Toshiro Matsui*

Cite This: *ACS Omega* 2025, 10, 7004−7012

Read Online

ACCESS | Metrics & More | Article Recommendations | Supporting Information

ABSTRACT: Ergothioneine (EGT), a naturally occurring histidine derivative, has been reported to modulate neurodegenerative diseases; however, the underlying mechanism remains unclear. This study aimed to investigate the brain-beneficial role of the natural amino acid EGT in NE-4C nerve cells. In the nerve cells, EGT treatment of >10 μM for 48 h significantly increased the expression of brain-derived neurotrophic factor (BDNF), as well as the phosphorylation of cAMP response element-binding protein (CREB), whereas no change was observed in acetylcholine receptor expression. Additionally, EGT induced an increase in intracellular Ca^{2+} levels via stimulation of the inositol 1,4,5-triphosphate receptor (IP_3R) in the endoplasmic reticulum; this increase was abrogated by the inhibition of organic cation transporter 1 (OCTN1). Structure−activity relationship analysis revealed the importance of the trimethylammonium group in EGT for intracellular events. In conclusion, EGT incorporated into cells via the OCTN1 route may act as a nerve transmission stimulator via IP_3R-mediated Ca^{2+}-CREB/BDNF activation.

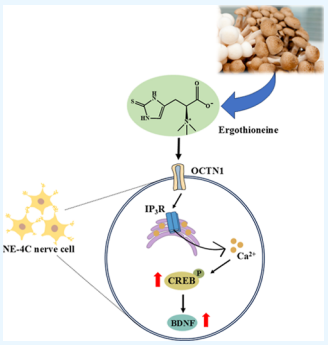

1. INTRODUCTION

Neurodegenerative diseases (NDDs), such as Alzheimer's disease (AD) and Parkinson's disease, are classified as neurological disorders characterized by the progressive loss of neurons in the central or peripheral nervous system.[1] Brain-derived neurotrophic factor (BDNF), a neurotrophin, has generated the most research interest due to its therapeutic potential for NDDs[2] because BDNF can ameliorate neuronal damage and promoted autophagy in SH-SY5Y cells[3] and BDNF mRNA expression was lower in the brain of AD patients, compared to individuals with no AD.[4] Therefore, the amelioration of the degraded BDNF signaling cascade is an alternative and appropriate strategy for the treatment or prevention of AD via diet because food compounds such as sulforaphane,[5] polyphenols,[6] peptides,[7] and fish oil[8] improved impaired cognition in animal studies mediated by BDNF activation.

Ergothioneine (EGT) is a naturally occurring sulfur-containing amino acid derived from histidine (His),[9] commonly found in mushrooms. For example, *Boletus edulis* and yellow oyster mushrooms contain EGT at 7.27 mg/g and 7.18 mg/g, respectively.[10] To date, EGT has attracted an increasing research attention owing to its physiological potential, including antioxidation,[11] antidiabetes,[12] and cardiovascular-protection,[13] in human studies. In addition to these health benefits, Song et al.[14] clarified that EGT intake in D-galactose-treated C57BL/6J mice activates the acetylcholine (ACh) nerve signaling pathways. Other reports also claimed the brain-health benefits of EGT with antiaging effect[15] by increasing synapsin I expression in hippocampal cells[16] and by eliminating senescent neuronal cells in hippocampus cells.[17] The beneficial effect of EGT on the brain can be attributed to intact transport across the blood−brain barrier (BBB) and accumulation in the mouse brain (10.66 ng/mg-brain[18]), possibly via organic cation transporter 1 (OCTN1).[19] In amyloid β $(A\beta)_{1-40}$-induced mouse models, brain-accessible EGT has been shown to prevent $A\beta$ accumulation in the hippocampus by reducing acetylcholinesterase (AChE) activity.[20] However, the underlying mechanism of brain-beneficial EGT in the nervous system remains unclear.

In the present study, we explored the potential neurotransmission mechanisms of EGT in NE-4C nerve cells that were derived from the cerebral vesicles of a p53 gene-deficient mouse embryo[21] because the cells possess ACh and BDNF nerve signaling systems targeted in this study.[22] The structure−activity relationship was also analyzed using EGT and the analogues. In this study, we used L-hercynine (ERY), His, and 2-mercapto-L-histidine (mer-His), as depicted in Figure 1. Although EGT has two tautomeric thiol and thioketone forms, the predominant EGT under physiological situation is a thioketone form (Figure 1).[23] ERY was selected because of the lack of a thioketone group in the EGT structure. Mer-His was also selected because of the lack of the trimethylammonium moiety in the EGT structure, even though the thioketone group in EGT was replaced with the thiol group.

Received: October 30, 2024
Revised: February 2, 2025
Accepted: February 5, 2025
Published: February 17, 2025

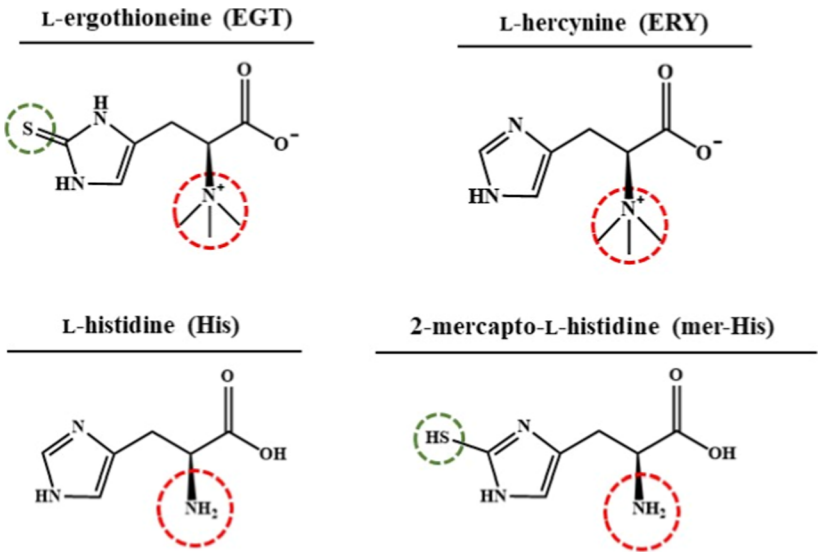

Figure 1. Structures of ergothioneine (EGT) and its analogues. (L-hercynine, ERY; L-histidine, His; and 2-mercapto-L-histidine, mer-His.

2. MATERIALS AND METHODS

2.1. Chemicals and Reagents. Eagle's minimal essential medium (E-MEM) and retinoic acid (RA; Lot: SKH3179) were obtained from FUJIFILM Wako Pure Chemical Co. (Osaka, Japan). Fetal bovine serum (FBS) was purchased from Corning (Glendale, AZ, USA). L-EGT (Lot: 5-NSR-167-2) was purchased from Toronto Research Chemicals, Inc. (Toronto, Ontario, Canada). Poly-L-lysine solution (PLL; Lot: RNBM2127), ERY (Lot: 0000219037), mer-His (Lot: B02860979), 2-aminoethyl diphenylborinate (2-APB; Lot: BCBT7914), and pyrilamine maleate salt (Lot: MKCS9706) were purchased from Sigma-Aldrich (St. Louis, MO, USA). His (Lot: M8T1362) was purchased from Nacalai Tesque Co. (Kyoto, Japan). Dantrolene sodium (Lot: S547802) was purchased from Selleck Chemical Co. (Tokyo, Japan). An intracellular Ca^{2+} determination kit (Calcium Kit II-Fluo 4; Lot: WQ064) was purchased from DOJINDO Laboratories (Kumamoto, Japan).

2.2. Cell Culture. The neural stem cell line NE-4C (CRL-2925, Lot: 70050986) was purchased from the American Type Culture Collection (Manassas, VA, USA). The stem cells were cultured in PLL-coated 75 cm^2 flasks in E-MEM medium (containing L-glutamine, phenol red, sodium pyruvate, nonessential amino acids, and 1500 mg/L sodium bicarbonate) supplemented with 10% FBS and 1% penicillin/streptomycin at 37 °C in a 95% air/5% CO_2 humidified incubator. The cells were dissociated using 0.05% trypsin and transferred to new flasks when the growth confluence reached to 80−90%. Fifth-passage cells were used for all of the experiments.

2.3. Preparation of NE-4C Cell Lysate for Protein Expression Assay. NE-4C stem cells (9×10^4 cells) were seeded in 35 mm PLL-coated dishes, followed by the addition of 1 μM RA in E-MEM containing 5% FBS for stem cell differentiation.[22] After 4 days incubation, the nerve cells were rinsed twice with warm phosphate-buffered saline solution and lysed with ice-cold 1× radioimmunoprecipitation assay (RIPA) buffer (50 mM Tris−HCl, 150 mM NaCl, 0.5% deoxycholic acid sodium salt, 0.1% sodium dodecyl sulfate, and 1% NP-40, pH 8.0) containing a protease (Nacalai Tesque Co.) and phosphatase (PhosSTOP, Roche, Basel, Switzerland) inhibitor cocktail tablets. After scraping, the obtained cell lysates were sonicated using Branson Digital Sonifier SFX 250 (Emerson Japan Co., Kanagawa, Japan) with an output control of 3 for 30 s at 4 °C, followed by centrifugation at 15,000*g* for 5 min at 4 °C (KUBOTA 3520, KUBOTA Co., Tokyo, Japan). An aliquot of the supernatant was used to determine the total protein concentration using the Pierce Protein Assay Kit (Lot: YG372899; Thermo Fisher Scientific, Waltham, MA, USA). The remaining supernatant was used for protein expression analysis via a Wes assay.

2.4. Measurement of Protein Expression by Wes. Protein expression levels were measured using a capillary electrophoresis-based immunoassay Wes instrument (ProteinSimple Co., San Jose, CA, USA) according to the manufacturer's instructions. Briefly, the supernatant was diluted to 0.5 mg/mL with 0.1× sample buffer and 5× fluorescent master mix denaturing buffer, followed by denaturation at 95 °C for 5 min using the PCR Thermal Cycler (Takara Bio Inc., Shiga, Japan). After denaturation, a sample solution, biotinylated Wes reagents, and primary antibodies were loaded onto a microplate, followed by centrifugation (TOMY AX-511, TOMY Digital Biology Co., Tokyo, Japan) at 2500 rpm for 5 min at 25 °C. Wes measurements were performed using a 12−230 kDa separation module (8 × 25 mm capillary cartridge, ProteinSimple Co.). Automatic immunodetection was performed by using a horseradish-peroxidase-conjugated secondary antibody and a chemiluminescent substrate. Total protein was detected by attaching a pentafluorophenyl ester-biotin labeling reagent to the applied proteins. The operating conditions of the Wes instrument were as follows: separation time, 28 min; separation voltage, 375 V; antibody dilution time, 30 min; primary antibody time, 60 min; and secondary antibody time, 30 min. The chemiluminescent signal was displayed as a virtual blot-like image or electropherogram using the Compass for SW software (ProteinSimple Co.). Protein expression was normalized to the electropherogram peak area of the corresponding total protein in each lane, and the data are expressed as a ratio to the control group. The primary antibodies used for immunoblotting were as follows: BDNF (anti-BDNF antibody, rabbit monoclonal antibody, Lot: 1035294-1, 1:50 dilution, Abcam, Cambridge, UK), phos-

https://doi.org/10.1021/acsomega.4c09920
ACS Omega 2025, 10, 7004−7012

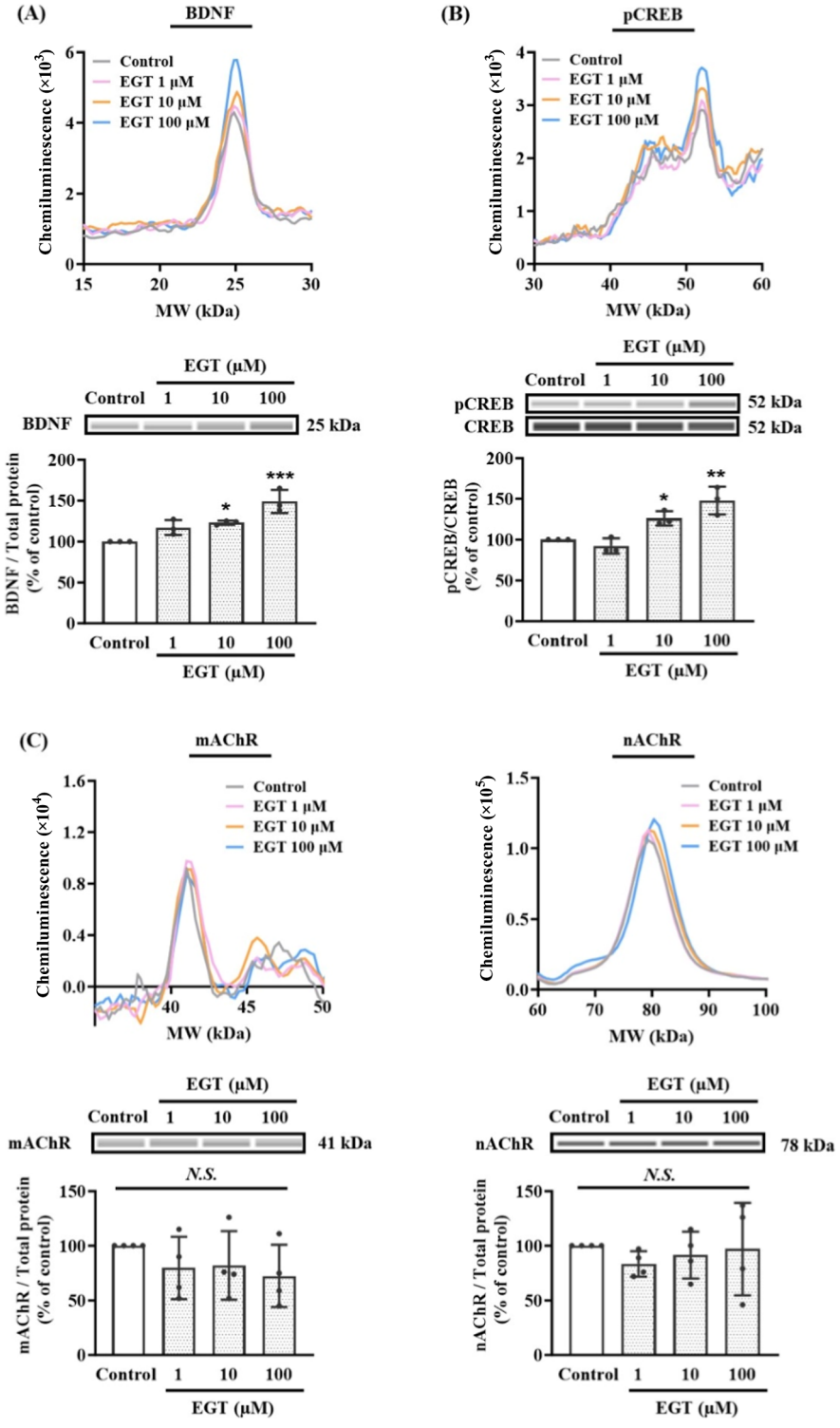

Figure 2. Effect of EGT on BDNF expression and CREB phosphorylation in NE-4C nerve cells. The expression of BDNF (A), ratio of pCREB and CREB (B), and m/n AChR (C) in NE-4C nerve cells treated with 1, 10, and 100 μM EGT were evaluated using Wes analysis. Protein expression of BDNF and m/n AChR was normalized using the electropherogram peak area of the total protein in each lane. The chemiluminescent signal was displayed as a virtual blot-like image, and an electropherogram was generated based on the molecular weight. Values are expressed as the mean ± SD (n = 3). Statistical analyses were performed using one-way ANOVA followed by Dunnett's t-test. *p < 0.05, **p < 0.01, ***p < 0.001 vs control; *N.S.*, no significance at p > 0.05.

pho-cAMP response element-binding protein (CREB) {pCREB (Ser133) [1B6], mouse monoclonal antibody, Lot: 11, 1:250 dilution, Cell Signaling Technology, Danvers, MA, USA}, CREB (anti-CREB antibody [D76D11], rabbit monoclonal antibody, Lot: 7, 1:50 dilution, Cell Signaling Technology), muscarinic AChR (anti-mAChR M1 antibody, Lot: 822203059, 1:50 dilution; GeneTex, CA, USA), and nicotinic AChR (anti-nAChR α4/CHRNA4 antibody, Lot: GR83312-9, 1:50 dilution; Abcam).

https://doi.org/10.1021/acsomega.4c09920
ACS Omega 2025, 10, 7004−7012

2.5. Measurement of Intracellular Ca^{2+} Levels in NE-4C Cells. The intracellular Ca^{2+} concentration ($[Ca^{2+}]_i$) was measured using a Flex Station 3 (Molecular Devices Co., San Jose, CA, USA) according to the manufacturer's instructions. Briefly, NE-4C stem cells seeded at a density of 3000 cells/well in a PLL-coated 96-well plate were used for this study. After differentiation with 1 μM RA, NE-4C nerve cells were incubated with a Fluo-4 AM loading buffer (100 μL/well, DOJINDO Laboratories) for 1 h at 37 °C in the dark. The loading buffer was formulated as follows: quenching buffer, Hanks' HEPES Buffer, 5% Pluronic F-127, 250 mM probenecid, and 0.9 mM Fluo-4 AM. After recording the basal fluorescence intensity (F_0) for 30 s, the sample solution containing EGT, ERY, His, or mer-His (20 μL) was added to each well through a multichannel pipettor of Flex Station 3 and the fluorescence intensity (arbitrary unit) was measured for 90 s to record the maximum fluorescence (F_{max}) signal. Change in relative Fluo-4 fluorescence or change in $[Ca^{2+}]_i$ (RFU, relative fluorescence unit) was expressed as $\Delta F = (F_{max} - F_0)$. For inhibitor experiments, $[Ca^{2+}]_i$ levels in cells were measured by adding 100 μM EGT solution containing either 2-APB (an inhibitor of 1,4,5-triphosphate receptor [IP_3R],[24] 10 μM) or dantrolene (an inhibitor of ryanodine receptor [RyR],[25] 10 μM). To evaluate the involvement of transporters in EGT-induced $[Ca^{2+}]_i$ change, pyrilamine (an antagonist of OCTN1,[26] 0.5 mM) or His (a substrate for PHT1 (peptide/histidine receptor 1), 100 μM) was used for $[Ca^{2+}]_i$ experiments. After the baseline fluorescence (F_0) signal was recorded for 30 s, a sample solution was added to each well through a multichannel pipet included as a part of the fluidics module of Flex Station 3.

2.6. Statistical Analysis. Data are expressed as the mean ± standard deviation (SD) of distinct replicates. All analyses were performed using GraphPad Prism software (version 10.0, GraphPad; La Jolla, CA, USA). Statistical differences between multiple groups were evaluated using one-way analysis of variance (ANOVA), followed by Dunnett's or Tukey's post hoc test. $p < 0.05$ was considered as a statistically significant difference.

3. RESULTS

3.1. Effect of EGT on BDNF Expression and CREB Phosphorylation in NE-4C Nerve Cells. A capillary electrophoresis-based immunoassay (Wes analysis) was performed to determine the effect of EGT on BDNF expression in NE-4C nerve cells. As shown in Figures 2A and S1, after a 2 day treatment of NE-4C progenitor cells with EGT, the expression of BDNF in the cells was significantly increased in a concentration-dependent manner (1−100 μM). Together with the increase in BDNF expression in NE-4C nerve cells, the expression of pCREB, an upstream signaling factor for BDNF generation,[27] was also increased by EGT (Figure 2B). This clearly suggested that EGT has physiological potential in stimulating CREB-mediated BDNF cascade in NE-4C nerve cells, similar to the upregulation of cascade by a food compound α-linolenic acid in PC12 cells.[28] Considering that m/n AChR expression was not affected by EGT (Figure 2C), the above finding may be due to an intracellular action of EGT within the cells.

3.2. Effect of EGT on $[Ca^{2+}]_i$ in NE-4C Nerve Cells. In the EGT-induced CREB-BDNF signaling, the mechanism of signaling activation by EGT remains a mystery. Since West et al.[29] reported that an increasing $[Ca^{2+}]_i$ was a trigger for phosphorylation of CREB in neurons, further experiments in EGT-treated NE-4C nerve cells focused on the changes in $[Ca^{2+}]_i$ at different concentrations of EGT (1, 10, and 100 μM). As shown in Figure 3, in situ Fluo-4-fluorescence Ca^{2+} measurements revealed a rapid elevation in $[Ca^{2+}]_i$ after EGT addition in a concentration-dependent manner (1−100 μM). These findings strongly suggest that EGT directly increases intracellular Ca^{2+} levels via extracellular or intracellular events. Because of a significant ($p < 0.0001$ vs control) increase in $[Ca^{2+}]_i$ by 100 μM EGT, this concentration was used for further Ca^{2+} experiments.

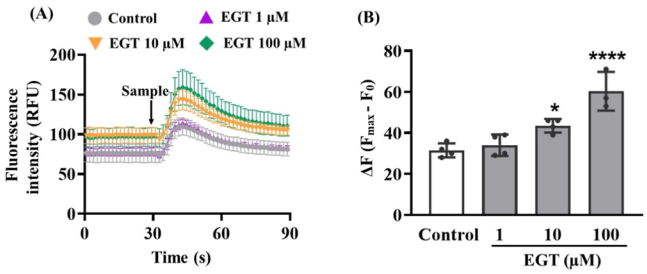

Figure 3. Effect of EGT on intracellular Ca^{2+} concentration ($[Ca^{2+}]_i$) in NE-4C nerve cells. (A) Real-time change of intracellular fluorescence signals with time in NE-4C nerve cells. The stimulation of EGT (1, 10, and 100 μM) started after 30 s of monitoring basal fluorescence intensity. (B) Transient changes of fluorescence from Fluo-4 after stimulation of EGT (1, 10, and 100 μM) in NE-4C nerve cells. Calcium kit II—Fluo 4 was used in this study. Transient changes in $[Ca^{2+}]_i$ [relative fluorescence units ,(RFU)] were calculated as the difference between peak (F_{max}) and basal (F_0) fluorescence intensity ($\Delta F = F_{max} - F_0$) at excitation wavelength of 485 nm, emission wavelength of 525 nm, and cutoff filter of 515 nm. RFU, relative fluorescence units. Values are expressed as the mean ± SD (n = 3 or 4). Statistical analyses were performed using one-way ANOVA followed by Dunnett's t-test. *$p < 0.05$, ****$p < 0.0001$ vs control.

3.3. Structure−Activity Relationship between EGT and Increase in $[Ca^{2+}]_i$ in NE-4C Nerve Cells. To assess the structural factors responsible for the EGT-induced increase in $[Ca^{2+}]_i$, EGT and its analogues (ERY, His, and mer-His) were subjected to $[Ca^{2+}]_i$ measurements in NE-4C nerve cells. As shown in Figure 4, EGT and ERY molecules, both of which have a trimethylammonium group, evoked a significant increase in $[Ca^{2+}]_i$, whereas no significant changes in $[Ca^{2+}]_i$ were observed with His or mer-His molecules, both of which lack this group. Structure−activity relationship analysis also revealed that the thioketone group in the imidazole moiety did not contribute to the observed increase in $[Ca^{2+}]_i$ by EGT (Figure 3). CREB phosphorylation and BDNF expression were also stimulated by EGT and ERY but not by His and mer-His (Figure S2), indicating that the trimethylammonium group is a key structural factor for the activation of the BDNF signaling cascade in NE-4C nerve cells.

3.4. Transport Route of EGT in NE-4C Nerve Cells. The transport routes of EGT in NE-4C nerve cells were investigated to clarify the increase in $[Ca^{2+}]_i$ via extracellular or intracellular events as a function of $[Ca^{2+}]_i$, using pyrilamine, an OCTN1 antagonist, and His, a substrate for PHT1. As shown in Figure 5, pyrilamine, but not His, significantly blocked the $[Ca^{2+}]_i$ elevation induced by EGT and ERY. This strongly suggests that the elevation of $[Ca^{2+}]_i$ by EGT (Figure 3), following the activation of CREB/BDNF signaling (Figure 2A,B), may be due to intracellular EGT being

https://doi.org/10.1021/acsomega.4c09920
ACS Omega 2025, 10, 7004−7012

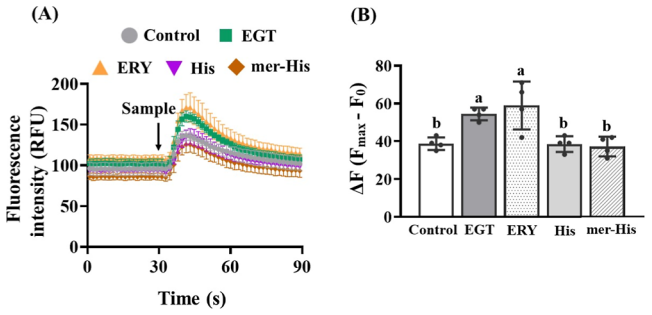

Figure 4. Structure−activity relationship achieved by contrasting the effect of EGT and its analogues on $[Ca^{2+}]_i$ in NE-4C nerve cells. (A) Real-time change of intracellular fluorescence signals with time in NE-4C nerve cells. The stimulation of sample (EGT, ERY, His, and mer-His) started after 30 s of monitoring basal fluorescence intensity. The concentration of each sample is 100 μM. (B) Transient changes of the intracellular fluorescence after sample stimulation in NE-4C nerve cells. Values are expressed as the mean ± SD (n = 4). Statistical analyses were performed using one-way ANOVA followed by Tukey−Kramer's t-test among multiple groups. Different letters represent the statistical difference at $p < 0.05$.

incorporated into NE-4C nerve cells via the OCTN1 transport route. This is consistent with a previous report indicating that EGT was incorporated into human embryonic kidney 293 cells through the OCTN1 transport route.[30]

3.5. Mechanism of EGT-Induced Increase in $[Ca^{2+}]_i$ in NE-4C Nerve Cells. Based on the above finding that the increase in $[Ca^{2+}]_i$ resulted from the incorporation of EGT into the cells, we focused on the release of Ca^{2+} from the endoplasmic reticulum (ER), which serves as a main dynamic Ca^{2+} storage organelle in cells.[31] When the Ca^{2+} released from the ER was blocked using inhibitors for IP_3R and RyR, which are intracellular Ca^{2+} channels,[32] inhibition of IP_3R by 2-APB significantly abolished EGT-induced $[Ca^{2+}]_i$ elevation; however, no changes were observed in $[Ca^{2+}]_i$ in EGT-treated NE-4C cells due to RyR inhibitor dantrolene (Figure 6). These results suggest that EGT and ERY molecules bearing a trimethylammonium group may act as IP_3R-specific stimulators or Ca^{2+} release promoters, leading to activation of the CREB/BDNF signaling pathway.

4. DISCUSSION

EGT, a natural amino acid derived from His, has been shown to exhibit a variety of physiological functions, including NDD prevention effect, in animals and humans.[11−13,20,33−35] Yang et al.[20] reported that the daily intake of EGT (2 mg/kg) in AD mice for 51 days ameliorated the $A\beta_{1-40}$-induced loss of memory and learning abilities by reduced $A\beta$ accumulation in the hippocampus. Nakamichi et al.[35] also provided the evidence that the oral intake of EGT (50 mg/kg, 2 weeks) enhances object recognition memory in normal ICR mice via the promotion of neuronal maturation. However, the mechanism underlying these effects of EGT is not fully understood.

This study, for the first time, provided evidence that EGT activates the CREB/BDNF pathway in NE-4C nerve cells (Figure 2A,B). Similarly, food compounds, such as sulforaphane,[5] α-linolenic acid,[28] lycopene,[36] and peptides,[37] have been reported as potential candidates for the upregulation of

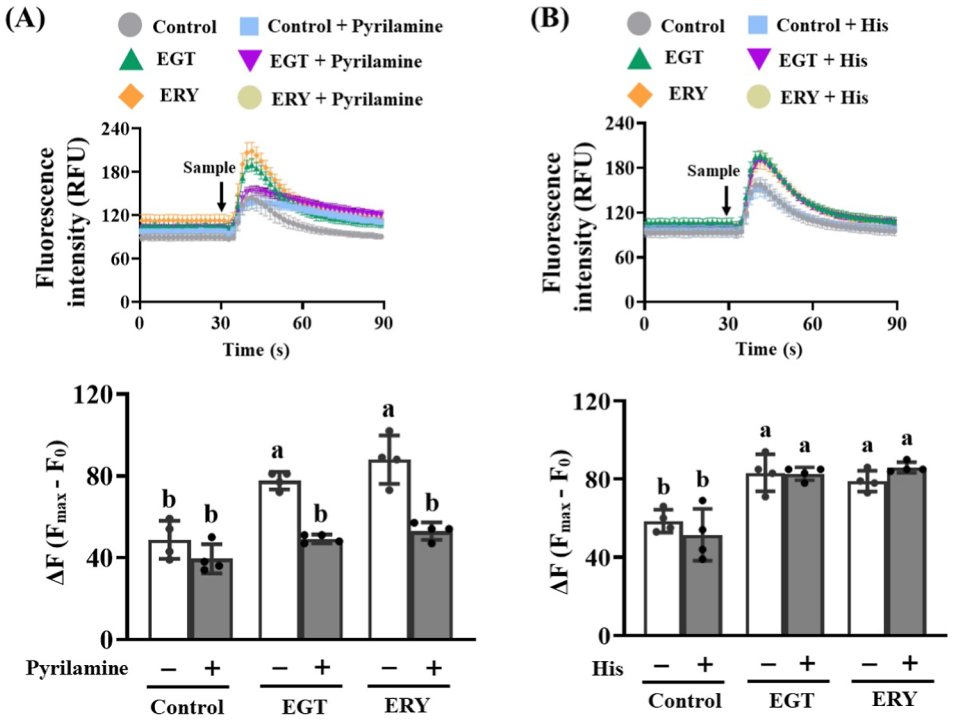

Figure 5. Involvement of OCTN1 and PHT1 in EGT-or ERY-induced Ca^{2+} release in NE-4C nerve cells. (A) Changes in $[Ca^{2+}]_i$ in NE-4C nerve cells treated with EGT or ERY (100 μM) in the presence or absence of pyrilamine (antagonist of OCTN1, 0.5 mM). (B) Alternations of $[Ca^{2+}]_i$ in NE-4C nerve cells treated with EGT or ERY (100 μM) with or without His (substrate of PHT1, 100 μM). After 30 s of monitoring basal fluorescence intensity, the prepared samples were added to NE-4C nerve cells. Values are expressed as the mean ± SD (n = 4). Statistical analyses were performed using one-way ANOVA followed by Tukey−Kramer's t-test among multiple groups. Different letters represent the statistical difference at $p < 0.05$. OCTN1, organic cation transporter 1; PHT1, peptide/histidine transporter 1.

https://doi.org/10.1021/acsomega.4c09920
ACS Omega 2025, 10, 7004−7012

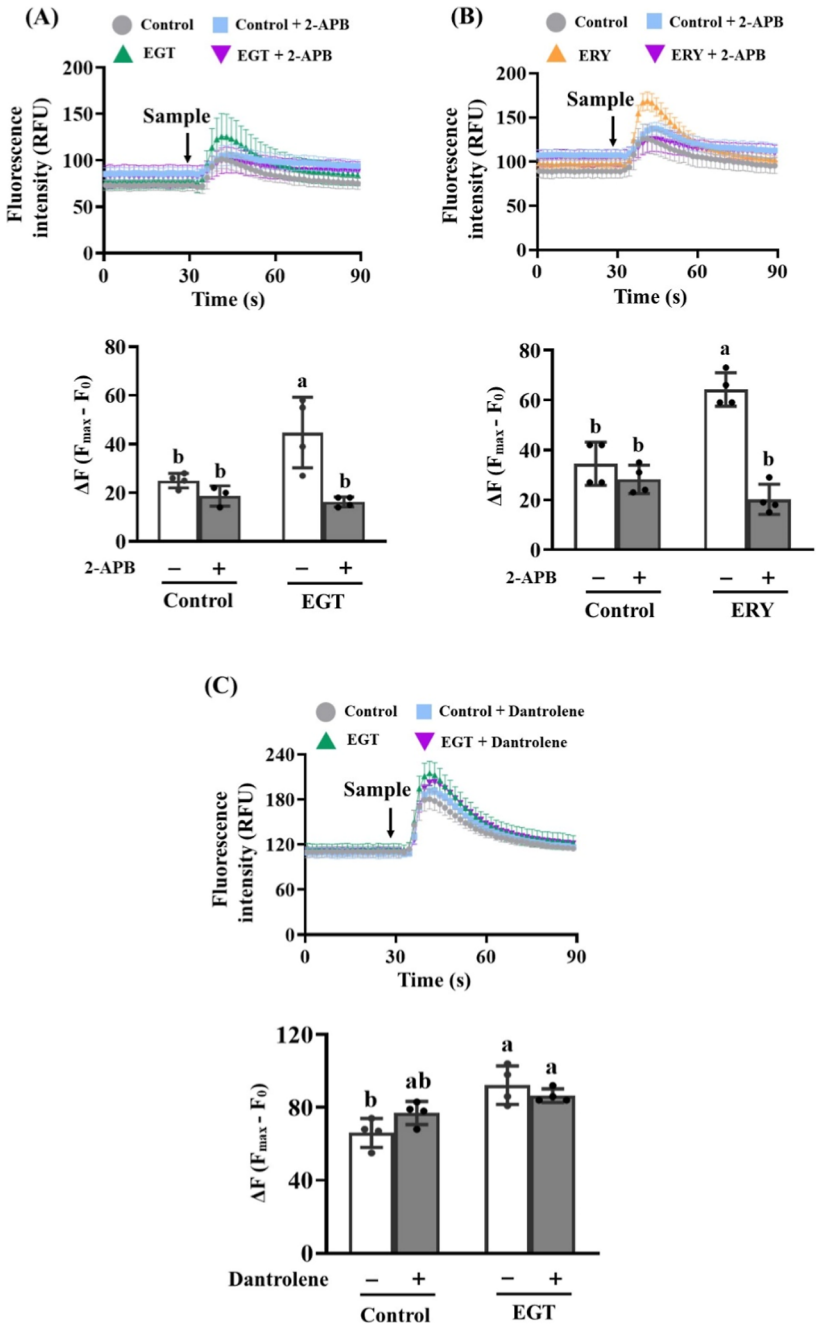

Figure 6. Effect of intracellular Ca^{2+} release channel on EGT-induced increase in $[Ca^{2+}]_i$ in NE-4C nerve cells. (A) Effect of 2-APB (inhibitor of IP_3R) on EGT-stimulated $[Ca^{2+}]_i$ changes in NE-4C nerve cells. (B) Impact of 2-APB on ERY-induced $[Ca^{2+}]_i$ increase in nerve cells. (C) Effect of dantrolene (inhibitor of RyR) on EGT-stimulated $[Ca^{2+}]_i$ upregulation in nerve cells. After 30 s of monitoring basal fluorescence intensity, the prepared samples were added to NE-4C nerve cells. Values are expressed as the mean ± SD (n = 3 or 4). Statistical analyses were performed using one-way ANOVA followed by Tukey−Kramer's t-test among multiple groups. Different letters represent the statistical difference at $p < 0.05$. 2-APB, 2-aminoethoxydiphenyl borate; IP_3R, inositol 1,4,5-trisphosphate receptor; RyR, ryanodine receptor. 2-APB, 10 μM; EGT, 100 μM; ERY, 100 μM; and dantrolene, 10 μM.

BDNF cascade. However, except for α-linolenic acid, which activated the protein kinase A (PKA)/CREB/BDNF signaling cascade in PC12 cells, the mechanism(s) underlying CREB/BDNF activation of the above food compounds remained unascertained. Considering the reported bioavailability[18] and a long stability (half-life, 1 month in rats[38]) of EGT, the intake would be a benefit for brain health, compared to the above neuroprotective compounds. BDNF is upregulated by the stimulation of transmembrane ACh receptors (m/n AChR) in the rat hippocampus and cerebral cortex.[39,40] However, in this study, EGT with a trimethylammonium group, such as ACh, did not affect m/n AChR expression (Figure 2C), suggesting that EGT-induced activation of the CREB/BDNF pathway (Figure 2) may be caused by an intracellular event and not AChR-mediated pathways.

For the stimulation of CREB/BDNF signaling, Ca^{2+} plays a crucial role in the activation of Ca^{2+}/calmodulin-dependent kinase II (CaMKII), p38 mitogen-activated protein kinase (MAPK)-mediated BDNF cascade,[41] and tyrosine receptor kinase B (TrkB)-mediated signaling pathway. Based on the

https://doi.org/10.1021/acsomega.4c09920
ACS Omega 2025, 10, 7004−7012

present findings that the increased BDNF expression was due to the incorporation of EGT via the OCNT1 route, a reported EGT transport route[30] (Figure 5A), we further aimed to clarify whether EGT affects intracellular Ca^{2+} levels. As shown in Figure 3, EGT significantly increased $[Ca^{2+}]_i$ in NE-4C nerve cells. Zhong et al.[42] reported that peoniflorin, a monoterpene glycoside isolated from herbal medicine, attenuated Aβ-induced neurotoxicity via maintenance of $[Ca^{2+}]_i$ homeostasis in the rat hippocampus. In addition, gastrodin, a bioactive compound derived from a Chinese herb, was also found to ameliorate memory impairment via modulation of the Ca^{2+}/CaMKII pathway in rats with vascular dementia.[43] Although the involvement of TrkB or p38-MAPK for Ca^{2+}-mediated CREB/BDNF activation remained unclear, intracellular Ca^{2+} elevation by the natural compounds including EGT may be a trigger for the activation of the CREB/BDNF cascade. To further investigate the structure−activity relationship (Figures 4 and S2) and $[Ca^{2+}]_i$ elevation experiments (Figure 6), we identified, for the first time, that the trimethylammonium group in EGT is a key structural component responsible for increasing $[Ca^{2+}]_i$ via IP_3R stimulation. This is in line with a report that trimethylamine *N*-oxide, a metabolic product of choline, enhances Ca^{2+} release from platelet stores by augmenting IP_3 signaling pathways.[44] Further studies are in progress to explore the interaction between the trimethylammonium group in EGT and the IP_3R protein in the ER using our previously reported CHARMM-GUI molecular docking analysis.[45]

In the current study, even though we provided the first finding that EGT has potential for the activation of the Ca^{2+}-CREB/BDNF signaling pathway in NE-4C nerve cells, the potential translation of these findings into in vivo animal and human models is an issue that cannot be ignored. Tang et al.[18] studied the tissue distribution of EGT after oral administration in C57BL6J mice (70 mg/kg/day, 28 days) and found that the concentration of EGT reached 840 μM and 10.66 ng/mg-brain in the mouse blood and brain tissue, respectively. In addition, in human administration study of mushroom-extract tablet containing 5 mg of EGT for 12 weeks, the concentration was estimated to be 497 μM in blood.[33] Taken together, the current results obtained at >10 μM of EGT would be acceptable under physiological conditions, but bioavailability analysis of EGT is still needed for further study. Considering the limitations of the current NE-4C cell model, the EGT-stimulated neurotransmission will be further explored in other neuronal cell models, such as SH-SY5Y cells[46] and Neuro-2a cells,[47] and in animal models, such as senescence-accelerated mouse model.[48] Besides, the synergistic effect of EGT with neuroprotective agents is also a promising and innovative research direction.

In conclusion, we demonstrated that EGT, a His metabolite commonly found in mushrooms[10] and *Aspergillus oryzae*-fermented rice bran,[49] stimulates neurotransmission via the IP_3R-mediated Ca^{2+}-CREB/BDNF signaling pathway in NE-4C nerve cells (Figure 7). The structure−activity studies revealed that the presence of the trimethylammonium group in EGT is essential for activity, while the thioketone group does not affect the activity. Additionally, considering the high bioavailability of EGT, it would be a brain-beneficial food compound across the BBB, like Tyr−Pro,[50] after oral diet of EGT or EGT-containing foods.

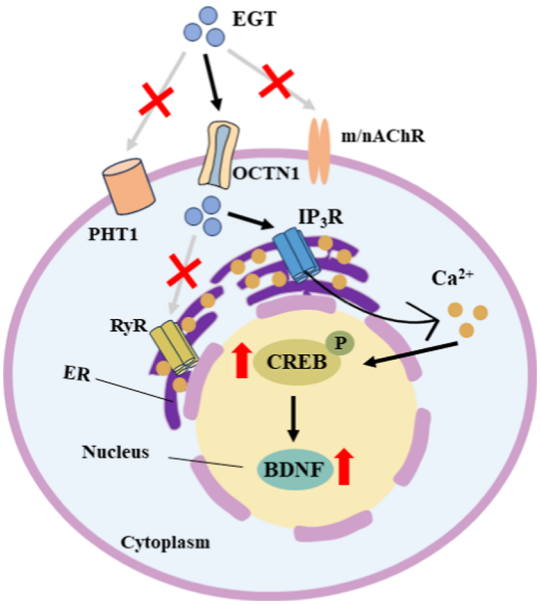

Figure 7. Schematic signaling pathway of EGT toward BDNF expression in NE-4C nerve cells.

■ ASSOCIATED CONTENT

Data Availability Statement

All data generated or analyzed during this study are included in this article and supplementary documents.

Supporting Information

The Supporting Information is available free of charge at https://pubs.acs.org/doi/10.1021/acsomega.4c09920.

Uncropped virtual blot-like images of BDNF, pCREB/CREB, and m/n AChR using the Wes analysis; NE-4C progenitor cells treated with EGT (1, 10, and 100 μM) for 48 h; uncropped virtual blot-like images of pCREB/CREB and BDNF using the Wes analysis; NE-4C progenitor cells treated with EGT and its analogues (ERY, His, and mer-His) at a concentration of 100 μM for 48 h (PDF)

■ AUTHOR INFORMATION

Corresponding Author

Toshiro Matsui − *Department of Bioscience and Biotechnology, Faculty of Agriculture, Graduate School of Kyushu University, Fukuoka 819-0395, Japan*; orcid.org/0000-0002-9137-8417; Phone: +81-92-802-4752; Email: tmatsui@agr.kyushu-u.ac.jp

Authors

Caiyue Shi − *Department of Bioscience and Biotechnology, Faculty of Agriculture, Graduate School of Kyushu University, Fukuoka 819-0395, Japan*

Sumire Asaba − *Department of Bioscience and Biotechnology, Faculty of Agriculture, Graduate School of Kyushu University, Fukuoka 819-0395, Japan*

Saya Nakamura − *Department of Bioscience and Biotechnology, Faculty of Agriculture, Graduate School of Kyushu University, Fukuoka 819-0395, Japan*

Complete contact information is available at: https://pubs.acs.org/10.1021/acsomega.4c09920

https://doi.org/10.1021/acsomega.4c09920
ACS Omega 2025, 10, 7004−7012

Author Contributions

C.S. and S.A. performed cell line experiments. C.S., S.A., S.N., and T.M. analyzed and discussed the results. C.S. drafted the original manuscript. S.N. and T.M. reviewed and edited the manuscript. T.M. designed and supervised the study. All authors have read and approved the final version of the manuscript for publication.

Notes

The authors declare no competing financial interest.

■ ACKNOWLEDGMENTS

This study was partially supported by JSPS KAKENHI [grant number JP21H04863 (T.M.)].

■ ABBREVIATIONS

ACh	acetylcholine
m/n AChR	muscarinic/nicotinic ACh receptor
2-APB	2-aminoethyl diphenylborinate
BBB	blood−brain barrier
AD	Alzheimer's disease
BDNF	brain-derived neurotrophic factor
CaMKII	Ca^{2+}/calmodulin-dependent kinase II
CREB	cAMP response element-binding protein
EGT	L-ergothioneine
E-MEM	Eagle's minimal essential medium
ER	endoplasmic reticulum
ERY	L-hercynine
FBS	fetal bovine serum
IP_3R	inositol 1,4,5-triphosphate receptor
MAPK	mitogen-activated protein kinase
MCI	mild cognitive impairment
mer-His	2-mercapto-L-histidine
NDD	neurodegenerative disease
NGF	nerve growth factor
NT	neurotrophin
OCTN1	organic cation transporter 1
PBS	phosphate-buffered saline
PD	Parkinson's disease
PHT1	peptide/histidine transporter 1
PKA	protein kinase A
PLL	poly L-lysine solution
RA	retinoic acid
RIPA	radioimmunoprecipitation assay
RyR	ryanodine receptor
RFU	relative fluorescence unit
TrkB	tyrosine receptor kinase B

■ REFERENCES

(1) Lamptey, R. N. L.; Chaulagain, B.; Trivedi, R.; Gothwal, A.; Layek, B.; Singh, J. A Review of the Common Neurodegenerative Disorders: Current Therapeutic Approaches and the Potential Role of Nanotherapeutics. *Int. J. Mol. Sci.* **2022**, *23* (3), 1851.

(2) Miranda-Lourenço, C.; Ribeiro-Rodrigues, L.; Fonseca-Gomes, J.; Tanqueiro, S. R.; Belo, R. F.; Ferreira, C. B.; Rei, N.; Ferreira-Manso, M.; de Almeida-Borlido, C.; Costa-Coelho, T.; Freitas, C. F.; Zavalko, S.; Mouro, F. M.; Sebastião, A. M.; Xapelli, S.; Rodrigues, T. M.; Diógenes, M. J. Challenges of BDNF-Based Therapies: From Common to Rare Diseases. *Pharmacol. Res.* **2020**, *162*, 105281.

(3) Geng, X.; Zou, Y.; Li, J.; Li, S.; Qi, R.; Yu, H.; Zhong, L. BDNF Alleviates Parkinson's Disease by Promoting STAT3 Phosphorylation and Regulating Neuronal Autophagy. *Cell Tissue Res.* **2023**, *393* (3), 455−470.

(4) Connor, B.; Young, D.; Yan, Q.; Faull, R. L. M.; Synek, B.; Dragunow, M. Brain-Derived Neurotrophic Factor Is Reduced in Alzheimer's Disease. *Brain Res. Mol. Brain Res.* **1997**, *49* (1−2), 71−81.

(5) Kim, J.; Lee, S.; Choi, B.-R.; Yang, H.; Hwang, Y.; Park, J. H. Y.; LaFerla, F. M.; Han, J.-S.; Lee, K. W.; Kim, J. Sulforaphane Epigenetically Enhances Neuronal BDNF Expression and TrkB Signaling Pathways. *Mol. Nutr. Food Res.* **2017**, *61* (2), 1600194.

(6) Shimada, Y.; Sato, Y.; Kumazoe, M.; Kitamura, R.; Fujimura, Y.; Tachibana, H. Myricetin Improves Cognitive Function in SAMP8-Mice and Upregulates Brain-Derived Neurotrophic Factor and Nerve Growth Factor. *Biochem. Biophys. Res. Commun.* **2022**, *616*, 33−40.

(7) Ju, D.-T.; K, A. K.; Kuo, W.-W.; Ho, T.-J.; Chang, R.-L.; Lin, W.-T.; Day, C. H.; Viswanadha, V. V. P.; Liao, P.-H.; Huang, C.-Y. Bioactive Peptide VHVV Upregulates the Long-Term Memory-Related Biomarkers in Adult Spontaneously Hypertensive Rats. *Int. J. Mol. Sci.* **2019**, *20* (12), 3069.

(8) dos Santos, F. V.; Targa, A. D. S.; Hammerschmidt, I.; Zanata, S. M.; Maia, F. G.; Visentainer, J. V.; Santos Junior, O. O.; da Costa, B. A.; Lagranha, C. J.; Ferraz, A. C. Fish Oil Supplementation Reverses Behavioral and Neurochemical Alterations Induced by Swimming Exercise in Rats. *Physiol. Behav.* **2018**, *194*, 95−102.

(9) Paul, B. D. Ergothioneine: A Stress Vitamin with Antiaging, Vascular, and Neuroprotective Roles? *Antioxid. Redox Signal.* **2022**, *36* (16−18), 1306−1317.

(10) Kalaras, M. D.; Richie, J. P.; Calcagnotto, A.; Beelman, R. B. Mushrooms: A Rich Source of the Antioxidants Ergothioneine and Glutathione. *Food Chem.* **2017**, *233*, 429−433.

(11) Cheah, I. K.; Tang, R. M. Y.; Yew, T. S. Z.; Lim, K. H. C.; Halliwell, B. Administration of Pure Ergothioneine to Healthy Human Subjects: Uptake, Metabolism, and Effects on Biomarkers of Oxidative Damage and Inflammation. *Antioxid. Redox Signal.* **2017**, *26* (5), 193−206.

(12) McElwain, C. J.; Musumeci, A.; Manna, S.; McCarthy, F. P.; McCarthy, C. M. L-Ergothioneine Reduces Mitochondrial-Driven NLRP3 Activation in Gestational Diabetes Mellitus. *J. Reprod. Immunol.* **2024**, *161*, 104171.

(13) Smith, E.; Ottosson, F.; Hellstrand, S.; Ericson, U.; Orho-Melander, M.; Fernandez, C.; Melander, O. Ergothioneine Is Associated with Reduced Mortality and Decreased Risk of Cardiovascular Disease. *Heart* **2020**, *106* (9), 691−697.

(14) Song, T.-Y.; Lin, H.-C.; Chen, C.-L.; Wu, J.-H.; Liao, J.-W.; Hu, M.-L. Ergothioneine and Melatonin Attenuate Oxidative Stress and Protect against Learning and Memory Deficits in C57BL/6J Mice Treated with D-Galactose. *Free Radic. Res.* **2014**, *48* (9), 1049−1060.

(15) Chen, L.; Zhang, L.; Ye, X.; Deng, Z.; Zhao, C. Ergothioneine and Its Congeners: Anti-Ageing Mechanisms and Pharmacophore Biosynthesis. *Protein Cell* **2024**, *15* (3), 191−206.

(16) Ishimoto, T.; Kato, Y. Ergothioneine in the Brain. *FEBS Lett.* **2022**, *596* (10), 1290−1298.

(17) Apparoo, Y.; Wei Phan, C.; Rani Kuppusamy, U.; Chan, E. W. C. Potential Role of Ergothioneine Rich Mushroom as Anti-Aging Candidate through Elimination of Neuronal Senescent Cells. *Brain Res.* **2024**, *1824*, 148693.

(18) Tang, R. M. Y.; Cheah, I. K.-M.; Yew, T. S. K.; Halliwell, B. Distribution and Accumulation of Dietary Ergothioneine and Its Metabolites in Mouse Tissues. *Sci. Rep.* **2018**, *8* (1), 1601.

(19) Nakamichi, N.; Taguchi, T.; Hosotani, H.; Wakayama, T.; Shimizu, T.; Sugiura, T.; Iseki, S.; Kato, Y. Functional Expression of Carnitine/Organic Cation Transporter OCTN1 in Mouse Brain Neurons: Possible Involvement in Neuronal Differentiation. *Neurochem. Int.* **2012**, *61* (7), 1121−1132.

(20) Yang, N.-C.; Lin, H.-C.; Wu, J.-H.; Ou, H.-C.; Chai, Y.-C.; Tseng, C.-Y.; Liao, J.-W.; Song, T.-Y. Ergothioneine Protects against Neuronal Injury Induced by β-Amyloid in Mice. *Food Chem. Toxicol.* **2012**, *50* (11), 3902−3911.

(21) Donehower, L. A.; Harvey, M.; Slagle, B. L.; McArthur, M. J.; Montgomery, C. A., Jr; Butel, J. S.; Bradley, A. Mice Deficient for p53 Are Developmentally Normal but Susceptible to Spontaneous Tumours. *Nature* **1992**, *356* (6366), 215−221.

https://doi.org/10.1021/acsomega.4c09920
ACS Omega 2025, 10, 7004−7012

(22) Cheng, L.; Shi, C.; Nakamura, S.; Esaki, N.; Ichiba, Y.; Tanaka, M.; Sakai, K.; Matsui, T. Adiponectin-Receptor Agonistic Dipeptide Tyr-Pro Stimulates the Acetylcholine Nervous System in NE-4C Cells. *J. Agric. Food Chem.* **2024**, *72* (13), 7121−7129.
(23) Yadan, J.-C. Matching Chemical Properties to Molecular Biological Activities Opens a New Perspective on L-Ergothioneine. *FEBS Lett.* **2022**, *596* (10), 1299−1312.
(24) Fernandes, H. S.; Popik, B.; de Oliveira Alvares, L. Effects of Hippocampal IP_3R Inhibition on Contextual Fear Memory Consolidation, Retrieval, Reconsolidation and Extinction. *Neurobiol. Learn. Mem.* **2022**, *188* (107587), 107587.
(25) Ovcjak, A.; Xiao, A.; Kim, J.-S.; Xu, B.; Szeto, V.; Turlova, E.; Abussaud, A.; Chen, N.-H.; Miller, S. P.; Sun, H.-S.; Feng, Z.-P. Ryanodine Receptor Inhibitor Dantrolene Reduces Hypoxic-Ischemic Brain Injury in Neonatal Mice. *Exp. Neurol.* **2022**, *351* (113985), 113985.
(26) Tucker, R. A. J.; Cheah, I. K.; Halliwell, B. Specificity of the Ergothioneine Transporter Natively Expressed in HeLa Cells. *Biochem. Biophys. Res. Commun.* **2019**, *513* (1), 22−27.
(27) Esvald, E.-E.; Tuvikene, J.; Sirp, A.; Patil, S.; Bramham, C. R.; Timmusk, T. CREB Family Transcription Factors Are Major Mediators of BDNF Transcriptional Autoregulation in Cortical Neurons. *J. Neurosci.* **2020**, *40* (7), 1405−1426.
(28) Liu, H.; Han, L.; Xia, X.; Xiang, X. α-Linolenic Acid Alleviates Aluminium Chloride-Induced Toxicity in PC12 Cells by Activation of PKA-CREB-BDNF Signaling Pathway. *Oil Crop Science* **2022**, *7* (2), 63−70.
(29) West, A. E.; Chen, W. G.; Dalva, M. B.; Dolmetsch, R. E.; Kornhauser, J. M.; Shaywitz, A. J.; Takasu, M. A.; Tao, X.; Greenberg, M. E. Calcium Regulation of Neuronal Gene Expression. *Proc. Natl. Acad. Sci. U.S.A.* **2001**, *98* (20), 11024−11031.
(30) Gründemann, D.; Harlfinger, S.; Golz, S.; Geerts, A.; Lazar, A.; Berkels, R.; Jung, N.; Rubbert, A.; Schömig, E. Discovery of the Ergothioneine Transporter. *Proc. Natl. Acad. Sci. U.S.A.* **2005**, *102* (14), 5256−5261.
(31) Schwarz, D. S.; Blower, M. D. The Endoplasmic Reticulum: Structure, Function and Response to Cellular Signaling. *Cell. Mol. Life Sci.* **2016**, *73* (1), 79−94.
(32) Ramírez, O. A.; Córdova, A.; Cerda, M.; Lobos, P.; Härtel, S.; Couve, A.; Hidalgo, C. Ryanodine Receptor-Mediated Ca^{2+} Release and Atlastin-2 GTPase Activity Contribute to IP_3-Induced Dendritic Ca^{2+} Signals in Primary Hippocampal Neurons. *Cell Calcium* **2021**, *96*, 102399.
(33) Watanabe, N.; Matsumoto, S.; Suzuki, M.; Fukaya, T.; Kato, Y.; Hashiya, N. Effect of Ergothioneine on the Cognitive Function Improvement in Healthy Volunteers and Mild Cognitive Impairment Subjects−A Randomized, Double-Blind, Parallel-Group Comparison Study. *Jpn. Pharmacol Ther* **2020**, *48*, 685−697.
(34) Zajac, I.; Kakoschke, N.; May-Zhang, L. The Effect of Ergothioneine Supplementation on Cognitive Function and Other Health-Related Outcomes in Older Adults with Subjective Memory Complaints. *Curr. Dev. Nutr.* **2024**, *8* (103219), 103219.
(35) Nakamichi, N.; Nakao, S.; Nishiyama, M.; Takeda, Y.; Ishimoto, T.; Masuo, Y.; Matsumoto, S.; Suzuki, M.; Kato, Y. Oral Administration of the Food-Derived Hydrophilic Antioxidant Ergothioneine Enhances Object Recognition Memory in Mice. *Curr. Mol. Pharmacol.* **2020**, *14* (2), 220−233.
(36) Li, F.; Xiang, H.; Lu, J.; Chen, Z.; Huang, C.; Yuan, X. Lycopene Ameliorates PTSD-like Behaviors in Mice and Rebalances the Neuroinflammatory Response and Oxidative Stress in the Brain. *Physiol. Behav.* **2020**, *224* (113026), 113026.
(37) Katayama, S.; Imai, R.; Sugiyama, H.; Nakamura, S. Oral Administration of Soy Peptides Suppresses Cognitive Decline by Induction of Neurotrophic Factors in SAMP8 Mice. *J. Agric. Food Chem.* **2014**, *62* (16), 3563−3569.
(38) Kawano, H.; Higuchi, F.; Mayumi, T.; Hama, T. Studies on Ergothioneine. VII. Some Effects of Ergothioneine on Glycolytic Metabolism in Red Blood Cells from Rats. *Chem. Pharm. Bull.* **1982**, *30* (7), 2611−2613.
(39) Liu, S.; Shi, D.; Sun, Z.; He, Y.; Yang, J.; Wang, G. M2-AChR Mediates Rapid Antidepressant Effects of Scopolamine through Activating the MTORC1-BDNF Signaling Pathway in the Medial Prefrontal Cortex. *Front. Psychiatry* **2021**, *12*, 601985.
(40) Johansson, J.; Formaggio, E.; Fumagalli, G.; Chiamulera, C. Choline Up-Regulates BDNF and down-Regulates TrkB Neurotrophin Receptor in Rat Cortical Cell Culture. *Neuroreport* **2009**, *20* (9), 828−832.
(41) Zhu, G.; Liu, Y.; Zhi, Y.; Jin, Y.; Li, J.; Shi, W.; Liu, Y.; Han, Y.; Yu, S.; Jiang, J.; Zhao, X. PKA- and Ca^{2+}-Dependent P38 MAPK/CREB Activation Protects against Manganese-Mediated Neuronal Apoptosis. *Toxicol. Lett.* **2019**, *309*, 10−19.
(42) Zhong, S.-Z.; Ge, Q.-H.; Li, Q.; Qu, R.; Ma, S.-P. Peoniflorin Attentuates Abeta((1−42))-Mediated Neurotoxicity by Regulating Calcium Homeostasis and Ameliorating Oxidative Stress in Hippocampus of Rats. *J. Neurol. Sci.* **2009**, *280* (1−2), 71−78.
(43) Chen, T.-T.; Zhou, X.; Xu, Y.-N.; Li, Y.; Wu, X.-Y.; Xiang, Q.; Fu, L.-Y.; Hu, X.-X.; Tao, L.; Shen, X.-C. Gastrodin Ameliorates Learning and Memory Impairment in Rats with Vascular Dementia by Promoting Autophagy Flux via Inhibition of the Ca^{2+}/CaMKII Signal Pathway. *Aging* **2021**, *13* (7), 9542−9565.
(44) Zhu, W.; Gregory, J. C.; Org, E.; Buffa, J. A.; Gupta, N.; Wang, Z.; Li, L.; Fu, X.; Wu, Y.; Mehrabian, M.; Sartor, R. B.; McIntyre, T. M.; Silverstein, R. L.; Tang, W. H. W.; DiDonato, J. A.; Brown, J. M.; Lusis, A. J.; Hazen, S. L. Gut Microbial Metabolite TMAO Enhances Platelet Hyperreactivity and Thrombosis Risk. *Cell* **2016**, *165* (1), 111−124.
(45) Lee, Y.; Nakano, A.; Nakamura, S.; Sakai, K.; Tanaka, M.; Sanematsu, K.; Shigemura, N.; Matsui, T. In Vitro and in Silico Characterization of Adiponectin-Receptor Agonist Dipeptides. *Npj Sci. Food* **2021**, *5* (1), 29.
(46) An, L.; Li, M.; Zou, C.; Wang, K.; Zhang, W.; Huang, X.; Wang, Y. Walnut Polyphenols and the Active Metabolite Urolithin A Improve Oxidative Damage in SH-SY5Y Cells by up-Regulating PKA/CREB/BDNF Signaling. *Food Funct.* **2023**, *14* (6), 2698−2709.
(47) Tremblay, R. G.; Sikorska, M.; Sandhu, J. K.; Lanthier, P.; Ribecco-Lutkiewicz, M.; Bani-Yaghoub, M. Differentiation of Mouse Neuro 2a Cells into Dopamine Neurons. *J. Neurosci. Methods* **2010**, *186* (1), 60−67.
(48) Li, X.; Ichiba, Y.; Watanabe, T.; Yoshino, A.; Cheng, L.; Nagasato, Y.; Takata, F.; Dohgu, S.; Iwasaki, K.; Tanaka, M.; Matsui, T. Preventive Effect of Tyr-Pro, a Blood-Brain Barrier Transportable Dipeptide, on Memory Impairment in SAMP8 Mice. *Npj Sci. Food* **2024**, *8* (1), 114.
(49) Horie, Y.; Goto, A.; Imamura, R.; Itoh, M.; Ikegawa, S.; Ogawa, S.; Higashi, T. Quantification of Ergothioneine in Aspergillus Oryzae-Fermented Rice Bran by a Newly-Developed LC/ESI-MS/MS Method. *Lebenson. Wiss. Technol.* **2020**, *118* (108812), 108812.
(50) Tanaka, M.; Kiyohara, H.; Yoshino, A.; Nakano, A.; Takata, F.; Dohgu, S.; Kataoka, Y.; Matsui, T. Brain-transportable soy dipeptide, Tyr-Pro, attenuates amyloid β peptide25-35-induced memory impairment in mice. *Npj Sci. Food* **2020**, *4* (1), 7.

https://doi.org/10.1021/acsomega.4c09920
ACS Omega 2025, 10, 7004−7012